BIOCHEMISTRY
including biophysical chemistry & molecular biology

Article

pubs.acs.org/biochemistry

ATP Acyl Phosphate Reactivity Reveals Native Conformations of Hsp90 Paralogs and Inhibitor Target Engagement

Brian E. Nordin, Yongsheng Liu, Arwin Aban, Heidi E. Brown, Jiangyue Wu, Anna K. Hainley, Jonathan S. Rosenblum, Tyzoon K. Nomanbhoy, and John W. Kozarich*

ActivX Biosciences, Inc., La Jolla, California 92037, United States

Supporting Information

ABSTRACT: Hsp90 is an ATP-dependent chaperone of widespread interest as a drug target. Here, using an LC-MS/MS chemoproteomics platform based on a lysine-reactive ATP acyl phosphate probe, several Hsp90 inhibitors were profiled in native cell lysates. Inhibitor specificities for all four human paralogs of Hsp90 were simultaneously monitored at their endogenous relative abundances. Equipotent inhibition of probe labeling in each paralog occurred at sites both proximal to and distal from bound ATP observed in Hsp90 cocrystal structures, suggesting that the ATP probe is assaying a native conformation not predicted by available structures. Inhibitor profiling against a comprehensive panel of protein kinases and other ATP-binding proteins detected in native cell lysates identified PMS2, a member of the GHKL ATPase superfamily as an off-target of NVP-AUY922 and radicicol. Because of the endogenously high levels of Hsp90 paralogs in typical cell lysates, the measured potency of inhibitors was weaker than published IC_{50} values. Significant inhibition of Hsp90 required inhibitor concentrations above a threshold where off-target activity was detectable. Direct on- and off-target engagement was measured by profiling lysates derived from cells treated with Hsp90 inhibitors. These studies also assessed the downstream cellular pathway effects of Hsp90 inhibition, including the down regulation of several known Hsp90 client proteins and some previously unknown client proteins. Overall, the ATP probe-based assay methodology enabled a broad characterization of Hsp90 inhibitor activity and specificity in native cell lysates.

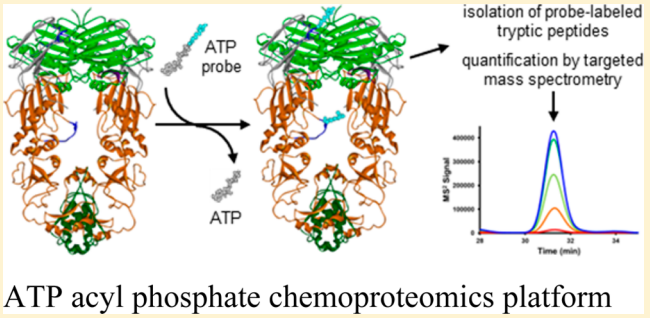

ATP acyl phosphate chemoproteomics platform

Chemical probes of enzyme active sites have proven to be invaluable tools for investigating several enzyme classes in a diverse range of biological settings.[1] We have previously described probes that link ATP to a desthiobiotin affinity tag through a reactive acyl phosphate bond. These probes covalently label lysine residues within the active sites of enzymes that recognize the ATP moiety, thereby allowing for the enrichment of tagged proteins on streptavidin-coated solid support. Alternatively, tagged proteins can be digested with proteases, and the isolated, labeled peptides can be identified and quantified using LC-MS/MS. By combining the proteomic scale of peptide mass spectrometry with an active-site-directed chemical probe, the inhibition status of several proteins derived from complex biological mixtures can be evaluated in a single experiment. A chemoproteomics LC-MS/MS platform, termed KiNativ, was developed using this methodology and is capable of quantifying several hundred probe-labeled peptides from protein kinase active sites.[2,3] The ATP probe also interacts with nucleotide binding sites from enzymes other than protein kinases. This has allowed us to significantly expand the scope of the profiling technology and apply it to the functional assessment of several classes of ATPases, including the prominent drug target Hsp90.

Heat shock protein 90 (Hsp90) is a highly conserved molecular chaperone that is abundantly expressed in a variety of organisms ranging from bacteria to yeast to humans.[4] It helps maintain the integrity of the proteome by coupling chemical energy from ATP hydrolysis to mechanical force used to drive the folding and maturation of substrate proteins, otherwise known as client proteins. Pharmacological inhibition of ATP binding to Hsp90 leads to the accumulation of improperly folded client proteins and their subsequent degradation through the ubiquitin−proteasome system.[5] Among the many known Hsp90 client proteins, there is a striking preponderance of protein kinases, steroid hormone receptors, and other proteins that have crucial roles in signal transduction pathways controlling cellular proliferation, differentiation, and the DNA-damage response.[6] Because these pathways are frequently deregulated in cancer, Hsp90 is the target of numerous oncology drug development efforts.

Hsp90 family members are dimeric enzymes consisting of three conserved domains: an N-terminal ATP-binding domain, a middle domain that assists in ATP hydrolysis, and a C-

Received: February 12, 2015
Revised: April 23, 2015
Published: April 23, 2015

DOI: 10.1021/acs.biochem.5b00148
Biochemistry 2015, 54, 3024−3036

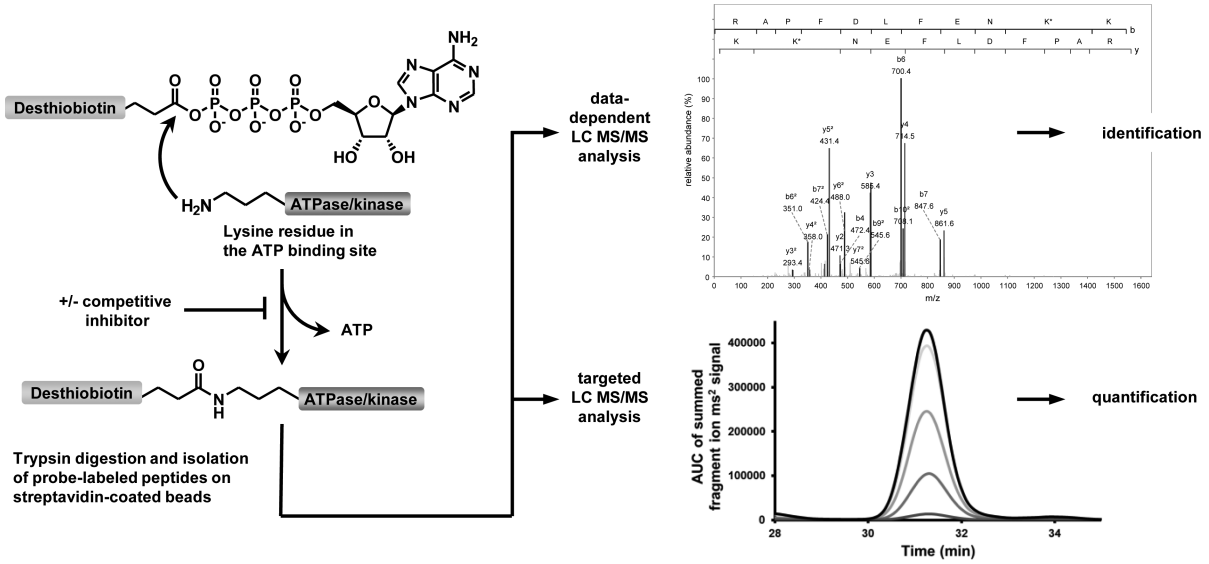

Figure 1. ATP acyl phosphate probe-based chemoproteomics. Lysine residues in ATP-binding sites are acylated with a desthiobiotin tag, and labeled peptides are isolated by affinity capture. The probe labeling reaction can be blocked by competitive inhibitors. Labeled peptides are identified on the basis of their ms^2 spectra generated by data-dependent LC-MS/MS. The AUC of summed fragment ion signal traces can be reliably quantified with targeted LC-MS/MS.

terminal dimerization domain. The ATP-binding domain adopts a unique tertiary structure, termed the Bergerat fold, also found in the DNA gyrase family, the DNA-mismatch-repair enzyme, MutL, and histidine kinases.[7] Collectively, these enzymes comprise the GHKL ATPase superfamily.[8] While each family shows no primary sequence homology to any of the other families, there is significant structural homology. Other than a variable, highly charged linker that connects the N-terminal and middle domains in eukaryotic (non-mitochondrial) Hsp90s, the gyrase, Hsp90 and MutL superfamily members all share the same basic organization of their three conserved domains. These three families also share a significant functional overlap in that they all couple ATP hydrolysis to large conformational changes.

While bacteria typically have a single, constitutively active Hsp90, humans and other mammals express four paralogs.[9] Hsp90α and Hsp90β are active in the cytosol, with Hsp90α being induced by stress and Hsp90β constitutively expressed. Grp94 is present in the endoplasmic reticulum, and Trap-1 is primarily located in the mitochondria. Initially, drug development efforts focused on cytosolic Hsp90 paralogs due to their involvement in the maturation of known oncogenes such as Her2, EGFR, Cdk4, and Raf-1. However, it has become clear that both Grp94 and Trap-1 play distinct roles in cancer and other diseases.[10] More recent drug development efforts have not only sought out inhibitors that are selective for either Grp94[11,12] or Trap-1,[13] but also placed greater emphasis on paralog specificity for Hsp90α/β. As more Hsp90 inhibitors progress through clinical trials it has become evident that some induce unacceptable toxicities, prompting the question of whether toxicities could be avoided with more specific inhibitors.[14]

Hsp90 interacts with several cochaperones and substrates throughout its catalytic cycle, many of which have significant effects on Hsp90 structure and activity.[15] Ideally, their effect on Hsp90 inhibitors should be accounted for in inhibition assays. Also, because many inhibitors bind to all four human Hsp90 paralogs, the ability to assess specificity is an important feature of an assay. Commonly used cellular assays that monitor protein abundance end points by antibody-based methods (e.g., Her2 degradation, Hsp70 induction) are capable of assaying inhibition in a setting where Hsp90 complexes with cochaperones are left intact. However, such assays generally cannot distinguish which Hsp90 paralog was responsible for mediating the observed effect. A variety of in vitro assays for measuring Hsp90 inhibition have been developed, some of which are suitable for determining paralog specificity, but attaining paralog specific information usually requires purified protein.[16] This negates the ability of the assay to account for the effects of cochaperones on Hsp90 activity.

Here, we use an ATP acyl phosphate probe to profile the ATP-binding sites of all four human Hsp90 family members in native cell lysates where protein−protein interactions remain intact. Through its capacity to be recognized by native Hsp90 paralogs in solution, it was found to covalently modify lysine residues that may only interact with bound ATP in a dynamic fashion, thereby providing evidence for previously unknown protein conformations. Several other types of ATP-binding proteins and protein kinases were concurrently assayed, allowing for Hsp90 inhibitor specificities to be broadly profiled. Additionally, when used to evaluate lysates derived from compound-treated cells, this technology was able to assess both direct inhibitor target engagement and downstream cellular effects of Hsp90 inhibition.

MATERIALS AND METHODS

Mass Spectrometry Sample Preparation. The materials and methods used to prepare samples for mass spectrometry have been described previously.[2,3] Except for two modifications to optimize ATPase profiling, the published methods were exactly replicated. First, the phosphatase inhibitor cocktail was excluded, as it was found to inhibit the labeling of a few ATPases. Second, we included 2 mM DTT in the probe labeling reactions to ensure that geldanamycin and 17-allylamino-17-desmethoxygeldanamycin (17-AAG) were reduced to their more potent hydroquinone forms. Geldanamy-

DOI: 10.1021/acs.biochem.5b00148
Biochemistry 2015, 54, 3024−3036

cin, 17-AAG, and radicicol were from AG Scientific. NVP-AUY922 and BIIB021 were from SelleckChem. For samples prepared with Asp-N protease (Roche), the method was the same as for trypsin except that Asp-N was added to a final concentration of 0.33 μg/mL and incubated for 20 h at 37 °C. The protease was then inactivated by adding SDS to a final concentration of 1% v/v.

Live Cell Treatment and FACS Analysis. MCF7 cells were cultured in MEME, 10% fetal calf serum. For A375 cells DMEM, 10% fetal calf serum was used. At an approximate cell density of 80% confluency, either inhibitor or DMSO was added to the final indicated concentration. After a 6 or 24 h duration, growth media was removed, and the cells were washed twice with 10 mL of cold PBS. Cells were harvested by manual scraping and pelleted by centrifugation. For each 100 μL of cell pellet a 900 μL volume of lysis buffer was added. Lysate was produced by sonication with a tip sonicator, and the resulting lysate was clarified by centrifugation at 16100*g* for 15 min. Cleared lysates were not gel-filtered in order to retain inhibitor, but otherwise processed like native cell lysate samples. For FACS analysis 20 μL of frozen cells were resuspended and lysed in a hypotonic buffer containing 50 μg/mL propidium iodide, 0.1% trisodium citrate dihydride, and 0.3 μL/mL Nonidet-P40. DNA staining was quantified on an Attune flow cytometer (Life Technologies), and data were analyzed using ModFit LT (Verity Software House).

LC-MS/MS Operation and Data Analysis. Mass spectrometry samples were run according to previously described methods with the exception that inclusion lists were specific to the needs of this study. Generally, protein kinase and ATPase inclusion lists were run from different injections of the same mass spectrometry sample. LTQ-Velos and LTQ-VelosPro mass spectrometers from Thermo Scientific were used interchangeably. Fragment ion extraction methods and signal quantification were exactly as previously published.

RESULTS

Chemoproteomic Profiling of ATP-Binding Enzymes Using an ATP Acyl Phosphate Probe. During the optimization of protein kinase profiling with the KiNativ platform, we identified a large number of peptides from other enzyme classes. Using this methodology, affinity-enriched, probe-labeled peptides are identified on the basis of their ms^2 fragmentation spectra collected in an ion trap mass spectrometer (Figure 1). Collecting ms^2 spectra for identification purposes is best accomplished by analyzing complex peptide mixtures in a "data-dependent" acquisition mode. However, this mode only yields parent ion ms^1 signal consistently over the duration of an LC-MS/MS run. For low abundance peptides the parent ion signal is not optimal and sometimes not even usable for quantification. A significantly greater amount of signal relative to background can be obtained by extracting characteristic fragment ion mass signals from ms^2 spectra derived from a known parent ion. Therefore, we used information (parent ion m/z values and elution times) obtained from data-dependent analyses to program the mass spectrometer to generate specific ms^2 spectra at defined times in a LC-MS/MS run. By running the mass spectrometer with an inclusion list (or "target list"), a reliable data sampling rate for each peptide target was obtained. Area under the curve (AUC) of summed fragment ion traces derived from targeted ms^2 spectra was quantified. Using this strategy we were able to reproducibly quantify several hundred peptides derived from ATP-binding enzymes outside of the protein kinase family, including all four human Hsp90 paralogs.

The reactive acyl phosphate moiety of the ATP probe preferentially acylates lysine side chains located in close proximity to the γ-phosphate of bound probe in enzyme active sites. The acylation reaction is competitively inhibited by other molecules capable of binding to the ATP site, e.g., free ATP itself and small molecule inhibitors. To a lesser degree the probe can also acylate lysines located on the surface of proteins or in regions of a protein that have general affinity for phosphate groups. These nonspecific acylation reactions likely follow second-order kinetics, as opposed to the pseudo-first-order kinetics followed by specifically bound probe, and are therefore mostly detectable for abundant proteins. Because we are interested in the occupancy of ATP-binding sites, we utilized competitive inhibition experiments with free ATP serving as inhibitor to distinguish specific probe labeling sites from nonspecific ones. Inhibition levels were measured as the loss of extracted fragment ion signal in inhibitor treated samples relative to control samples. As is the case for protein kinases, some ATP-binding enzymes belong to large families that share conserved, well annotated primary sequence motifs responsible for ATP binding (e.g., AAA+ ATPases, ABC transporters); however, this is not the case for all such enzymes. We observed dose-dependent inhibition of probe labeling by ATP at both well annotated ATP sites and at sites we may not have recognized as ATP-binding motifs based on primary sequence information alone. Some peptides failed to show inhibition, and generally, when these sequences were analyzed retrospectively using available crystal structures, the modified lysine residues were observed to be on the protein surface and not in an ATP-binding site.

In total, a combination of competitive inhibition experiments and mining of our internal database (for peptides with recognizable ATP-binding sequence motifs) led to the development of a target panel containing almost 300 probe-labeled human peptides that are sensitive to inhibition by free ATP (for a complete list see Figure S1, Supporting Information). A single MS run is sufficient to collect data on all of these target peptides, although in practice we generally observe that lysates derived from any single human cell line tend to yield quantifiable signal for 200−250 peptides (due to cell type specific expression). Several classes of enzymes are profiled in this panel including AAA+ ATPases, ABC transporters, aminoacyl-tRNA synthetases, actins, ATP-grasp domain containing enzymes, ATP-dependent helicases, Hsp60, Hsp70, Hsp90, myosins, nudix hydrolases, ubiquitin-activating enzymes, several types of small molecule kinases, and a variety of ATPases that do not belong to larger enzyme families. Largely, the enzymes identified by this work are known to bind ATP, and where crystal structures are available the acylated lysine residue is in close proximity to the ATP-binding site. A small number of the identified enzymes bind related nucleotides like NAD or FAD. Additionally, a few ATP-competitive probe labeling sites were identified from proteins that have no known nucleotide binding site; however, these examples are beyond the scope of this report.

ATP Probe Labeling Sites in Hsp90 Paralogs. Upon reviewing the ATP-sensitive peptides from Hsp90 paralogs selected for the human ATPase profiling panel, we noticed that they were not all located in the annotated ATP-binding domain. For each paralog, there were labeled peptides identified from both the N-terminal ATP-binding domain and

DOI: 10.1021/acs.biochem.5b00148
Biochemistry 2015, 54, 3024−3036

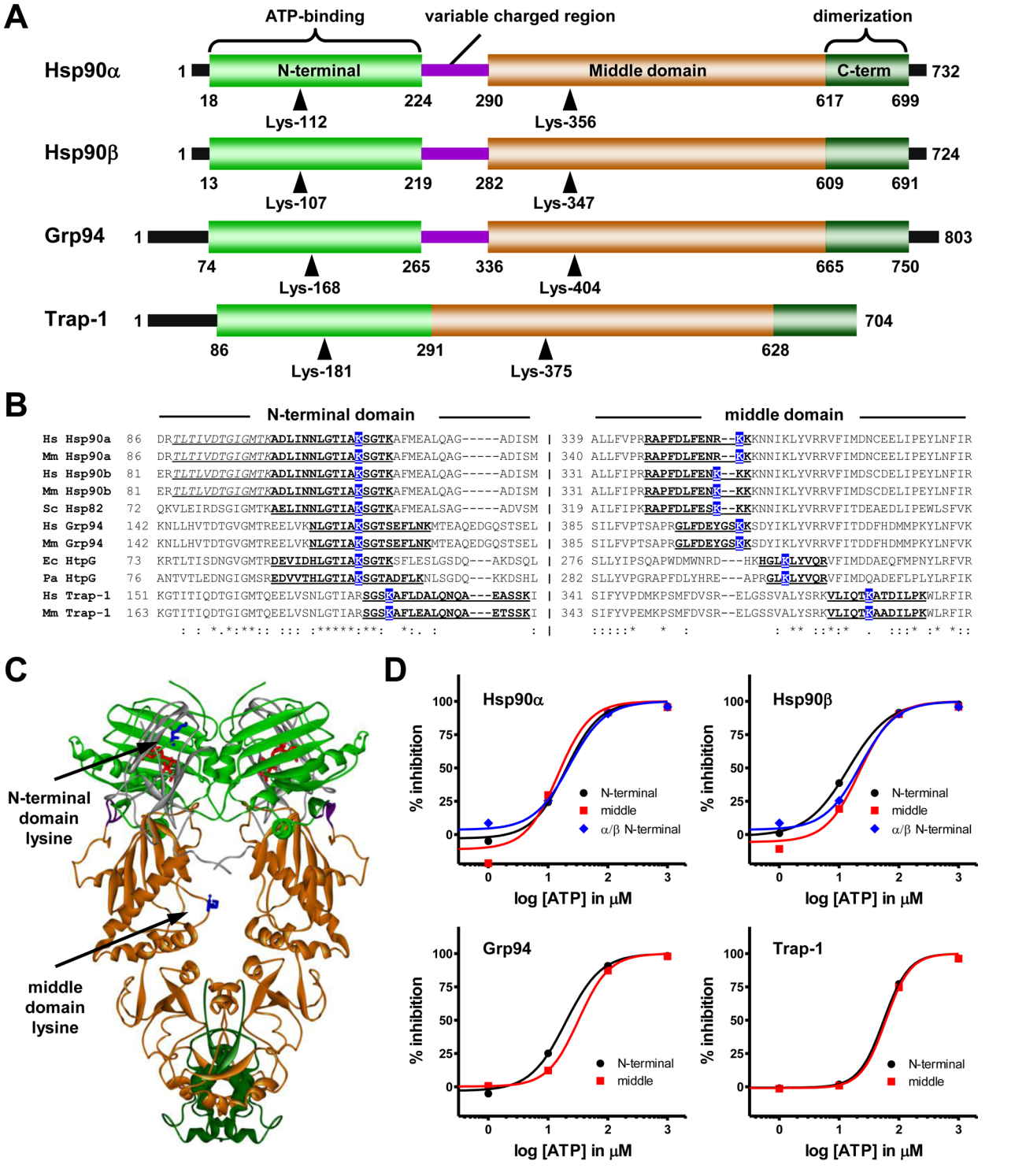

Figure 2. ATP probe labeling of Hsp90 paralogs. (A) Hsp90 family members are comprised of three domains; an N-terminal ATP binding domain (light green), a middle domain (orange), and a C-terminal dimerization domain (dark green). A poorly conserved, highly charged linker connects the N-terminal and middle domains of each paralog, except Trap-1. All four paralogs are labeled on the lysine residues within their N-terminal and middle domains indicated by the inverted triangles. (B) Multiple sequence alignment of Hsp90 paralogs that have been evaluated for ATP probe labeling. Both the N-terminal and middle domain regions where probe labeling was observed show significant primary sequence conservation. Observed tryptic peptides are underlined. The labeled lysine is shown in white font with blue highlight. The portion of the peptides resulting from missed cleavage events in Hsp90*α* and Hsp90*β* that allow for their unique identification is in italics. Hs - human, Mm - mouse, Sc - yeast, Ec - *E. coli*, Pa - *P. aeruginosa* (C) The full-length yeast Hsp90:Sba1:AMPPNP structure (PDB ID 2CG9) places the middle domain probe-labeling site more than 30 Å distant from the bound ATP analogue. The loop containing this site is only ordered in one of the two protomers. Domains of Hsp90 are colored as in (A). Sba1 is shown in gray. AMPPNP is red and the indicated lysines are blue. (D) Equipotent inhibition of probe labeling of N-terminal and middle domain peptides by ATP in native A375 lysate. Data from the Hsp90*α*/*β* redundant peptide showed the same dose response as either paralog-specific peptide. See Figure S2, Supporting Information for IC_{50} values.

DOI: 10.1021/acs.biochem.5b00148
Biochemistry 2015, 54, 3024−3036

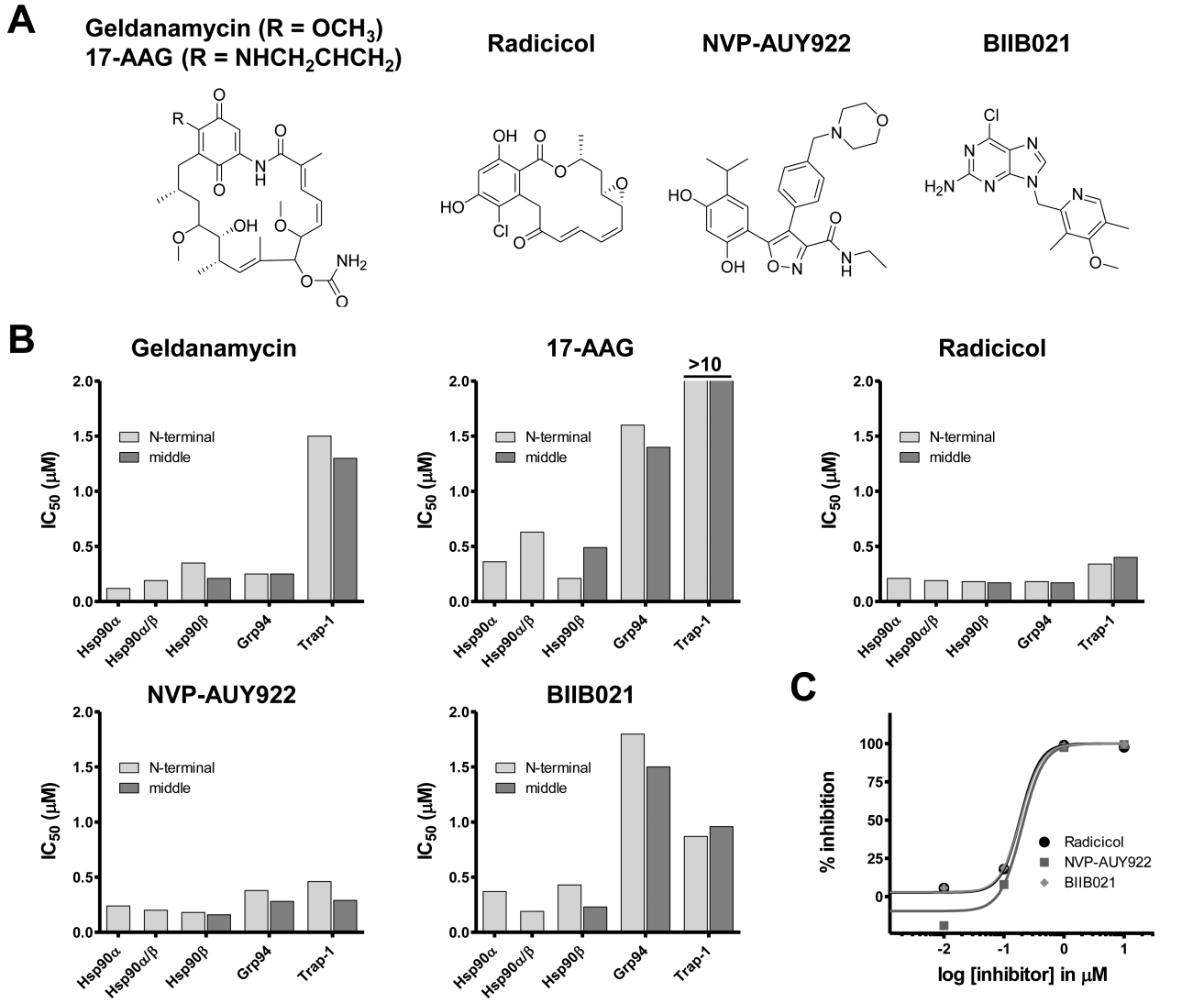

Figure 3. Hsp90 inhibitor paralog specificity. (A) Chemical structures of Hsp90 inhibitors used in this study. (B) Profiling of Hsp90 inhibitors in native A375 lysate revealed differing levels of paralog specificity. Equipotent inhibition was observed for both N-terminal and middle domain labeling. Hsp90α/β indicates the peptide redundant to both paralogs. (Low signal for the Hsp90α middle domain tryptic peptide prevented precise quantification in this experiment.) (C) Example dose response curves for the labeling of the Hsp90α/β N-terminal domain peptide. The Hsp90 inhibitors showed very high inhibition (>97%) at 1 μM, but relatively little inhibition (<20%) at 100 nM. See Figure S4, Supporting Information for the complete dose response data and IC_{50} values.

the middle domain that showed robust competitive inhibition by free ATP. The primary labeling sites for Hsp90α and Hsp90β in their N-terminal domains are Lys-112 and Lys-107, respectively (Figure 2A). While the fully trypsinized peptide sequences produced by Hsp90α and Hsp90β at this site are identical and therefore indistinguishable by mass spectrometry, a missed cleavage event at the N-terminal tryptic site of either peptide can yield sequences that are unique to each paralog. (See italicized sequences in Figure 2B. Also, note that the labeling of lysine by the probe prevents tryptic cleavage at that position.) On the basis of crystal structures of the isolated N-terminal domains in complex with nucleotides or inhibitors, the labeling of Lys-112 or Lys-107 is readily understood given their location within the ATP-binding site.[17] The same is true for the probe labeling of Lys-168 in Grp94 and Lys-181 in Trap-1 in their respective N-terminal ATP-binding domains. As seen in the multiple sequence alignment, these labeling sites all map to a region of the Hsp90 ATP-binding site that is not only conserved across the four human paralogs, but also in mice and evolutionarily distant bacterial and yeast species (Figure 2B). In fact, the analysis of proteomes from *Escherichia coli*, *Pseudomonas aeruginosa*, and *Saccharomyces cerevisiae* demonstrated that the equivalent lysine residues (highlighted in blue) were all acylated by the ATP probe.

All four human Hsp90 paralogs also demonstrated ATP-sensitive probe labeling in a segment of the middle domain. The observed labeling sites are clustered around Lys-356 of Hsp90α, a region of consecutive positively charged amino acids in Hsp90α, Hsp90β, and Grp94. Trap-1, the most evolutionarily distant of the four human Hsp90 paralogs, does not have a lysine or consecutive lysines at this position, but was found to be labeled at Lys-375, which aligns just downstream of the other labeling sites. Bacterial Hsp90s from *E. coli* and *P. aeruginosa* also showed middle domain labeling sites in a segment similar to that of Trap-1. These probe labeling events are not readily explainable considering the available, albeit very limited, structural information. As seen in Figure 2C, when mapped onto the structure of the full-length yeast Hsp90,[18] the

DOI: 10.1021/acs.biochem.5b00148
Biochemistry 2015, 54, 3024−3036

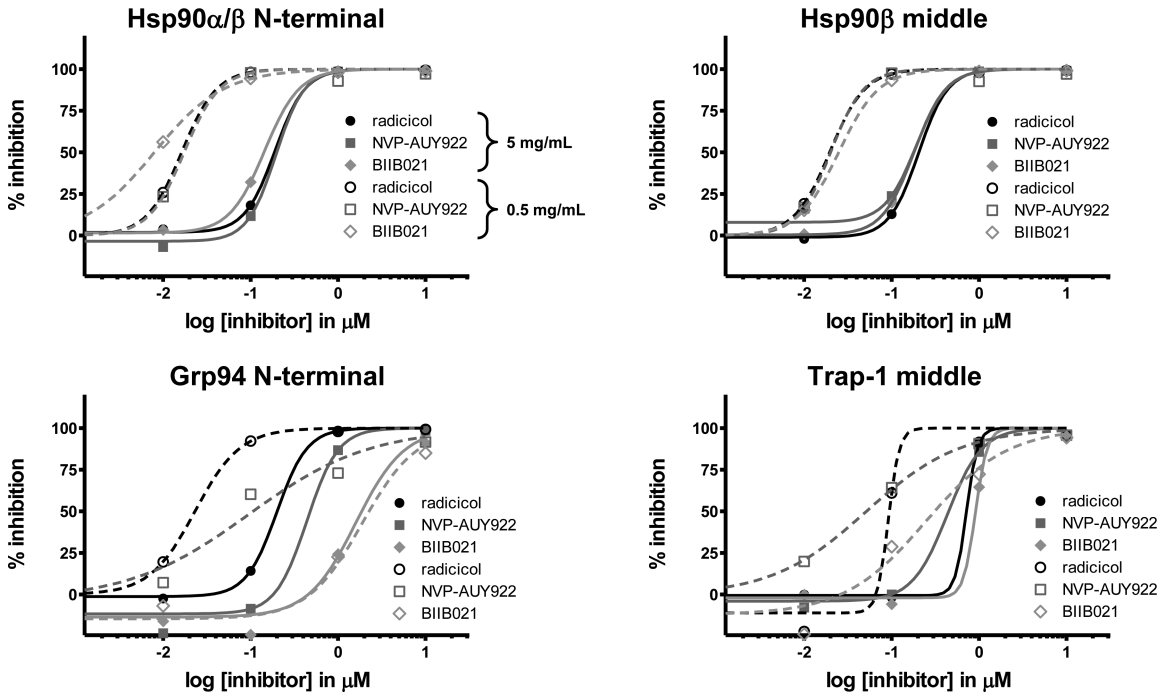

Figure 4. Influence of Hsp90 abundance on observed inhibitor potency. Three Hsp90 inhibitors were profiled in HL60 lysates with a total protein concentration of either 5 mg/mL (filled symbols, solid lines) or 0.5 mg/mL (open symbols, dashed lines). The observed shifts in potency revealed that the lower inhibitor concentrations were below the total Hsp90 paralog concentration. See also Figure S5, Supporting Information.

labeled middle domain lysine residue is not located near the ATP-binding site. Nonetheless, not only did all Hsp90 paralogs demonstrate inhibition by ATP at both their N-terminal and middle domain labeling sites, the IC_{50} values for both sites of each protein were equivalent (Figure 2D).

The labeled middle domain peptides derived from Hsp90*α* and Hsp90*β* differ only in the first position of a stretch of four consecutive positively charged amino acids; the arginine at position 355 in Hsp90*α* is a lysine in Hsp90*β* (see Figure 2B). For Hsp90*β*, this lysine (Lys-347) was identified as the most prominent middle domain labeling site. It yielded significantly more signal (>100-fold) than the equivalent peptide from Hsp90*α*, which generally gave a signal near the limit of detection. This difference was not consistent with the finding that the N-terminal domain peptides unique to Hsp90*α* and Hsp90*β* gave an approximately equal signal. To more thoroughly investigate the labeling of the middle domain of Hsp90*α*, we used the chemoproteomics platform to analyze peptides produced by the protease Asp-N, which leaves the stretches of consecutive arginine and lysine residues intact, unlike trypsin. This allowed for a direct comparison of labeling intensity among the stretch of consecutive lysine residues. The results revealed that probe labeling of both Hsp90*β* and Hsp90*α* was distributed among the multiple lysine positions with the most N-terminal positions giving the strongest signal. While the Hsp90*β* peptide labeled at Lys-347 gave about 20-fold more signal than that of the Hsp90*α* peptide labeled on Lys-356, the direct Hsp90*β* equivalent (labeled at Lys-348) gave only 3-fold more signal. This suggests that the first positively charged amino acid in each paralog is optimally positioned to interact with ATP, and the discrepancy in signal between the middle domain tryptic peptides of Hsp90*α* and Hsp90*β* occurs because Arg-355 of Hsp90*α* cannot be acylated. A more detailed discussion is presented in the Supporting Information (Figure S3).

Profiling Hsp90 Inhibitor Paralog Specificity. To further explore labeling sites in Hsp90 paralogs, we assessed the ability of known Hsp90 inhibitors to block the probe labeling reaction. We measured inhibition in native A375 lysates by a variety of compounds (Figure 3A) over a concentration range of 10 μM to 10 nM. The tested inhibitors included the natural products geldanamycin and radicicol, a semisynthetic compound, 17-AAG, and two compounds derived from pharmaceutical screening efforts, NVP-AUY922 and BIIB021. Despite their structural differences, all of these compounds function by competing with ATP for binding to the ATP site within the N-terminal domain of Hsp90 paralogs. The precise location and reversible mode of binding for each inhibitor (or a closely related analogue; i.e., geldanamycin for 17-AAG[17] and an earlier lead compound for NVP-AUY922[19]) has been confirmed through X-ray crystallographic analysis of cocrystal structures.[20,21] Like ATP itself, each compound inhibited probe labeling of both domains in a dose-dependent manner (Figure 3B). These data revealed clear differences in both overall potency and paralog specificity among the set of compounds. The two ansamycin derivatives, geldanamycin and 17-AAG, were much less potent against Trap-1 than they were against the other three paralogs. Also, the overall potency of 17-AAG was much lower than that of geldanamycin. Radicicol potently inhibited all four Hsp90 paralogs demonstrating very little selectivity. The paralog selectivity of NVP-AUY922 was modest with both Grp94 and Trap-1 showing slightly lower levels of inhibition. In contrast, BIIB021 demonstrated a greater degree of selectivity for the cytosolic Hsp90 paralogs, Hsp90*α* and Hsp90*β*, while having less activity toward Trap-1 and even less activity toward Grp94.

This method reproducibly yielded data indicating less potent inhibition than observed in previous studies using purified proteins. For example, the published IC_{50} values for NVP-AUY922 and BIIB021 in fluorescence polarization equilibrium

DOI: 10.1021/acs.biochem.5b00148
Biochemistry 2015, 54, 3024−3036

binding assays against Hsp90α are 7.8 nM and 1.7 nM, respectively,[22,23] whereas our data gave values of about 200 nM for both compounds. For all compounds published values were more potent than those derived from this experiment. The near complete absence of inhibition observed for these compounds at a concentration of 100 nM relative to that seen at a 1 μM concentration suggested that the aggregate concentration of Hsp90 paralogs was greater than 100 nM (Figure 3C). Our standard methods utilize cell lysates adjusted to a protein concentration of 5 mg/mL, and under these conditions we are able to detect labeled peptides from a wide variety of enzymes, including ones from low abundance proteins. We repeated the profiling experiment for three of the inhibitors using cell lysates at 5 and 0.5 mg/mL protein concentrations. As seen in Figure 4, the 10-fold reduction in protein concentration resulted in roughly a 10-fold shift toward increased inhibitor potency. Therefore, while all of the percent inhibition values are accurate, under our standard conditions we were titrating the total concentration of Hsp90 paralogs with inhibitor.

As was observed for the inhibition potency of ATP, specific Hsp90 inhibitors showed equal potency against both the N-terminal and middle domain labeling sites of any one paralog (Figure 3B). For example, BIIB021 showed potent inhibition of Hsp90α and Hsp90β for both N-terminal and middle domain peptides, while it demonstrated more moderate inhibition of Grp94 and Trap-1 on each of their respective labeling sites. This correlation of inhibition potencies was maintained at both of the proteome concentrations we analyzed. Taken as a whole, the ATP and inhibitor dose responses indicate that the probe labeling reactions of both the N-terminal domain and the middle domain are mediated by ATP probe bound at a single site.

Off-Target Inhibition by Hsp90 Inhibitors. One of the most useful features of the chemoproteomics platform is that inhibitors can be simultaneously profiled against both known targets and unknown potential targets. To search for possible off-targets of the Hsp90 inhibitors, we profiled the compounds against both a panel of ATPases that included the Hsp90 paralogs and an extensive panel of protein kinases. Combined, these panels produced quantitative data for about 500 probe-labeled peptides corresponding to nearly 400 enzymes. Separate LC-MS/MS runs were performed for each panel to maximize data sampling rates; however, individual mass spectrometry sample preparations are sufficient for multiple LC-MS/MS runs. Our results using A375 cellular lysates produced data on 255 probe labeling sites from about 205 protein kinases, none of which were significantly inhibited by any of the Hsp90 inhibitors (Figure S6A, Supporting Information).

The ATPase panel gave inhibition data on 222 active site peptides from 188 proteins in A375 lysates (Figure S6B, Supporting Information). Other than the four Hsp90 paralogs, only one other GHKL superfamily member was detected in this proteome. The human genome contains a limited number of other superfamily members, namely, two topoisomerases, five histidine kinases, and four MutL homologues. The MutL family member PMS2 gave a fairly weak signal for a peptide labeled on Lys-91, part of a highly conserved TSK tripeptide sequence known to interact with ATP.[8] These data clearly demonstrated that geldanamycin, 17-AAG, and BIIB021 did not inhibit PMS2 labeling; however, high signal variability among the radicicol samples prevented a statistically significant conclusion for this compound. NVP-AUY922 showed dose-dependent inhibition of PMS2, giving an IC_{50} value of approximately 1 μM (Figure S6B, Supporting Information). We repeated the ATPase panel for three of the compounds, this time using a HeLa cell lysate, which was found to give a stronger PMS2 signal. Here we clearly observed that both NVP-AUY922 and radicicol inhibit the probe labeling of PMS2, where BIIB021 again did not (Figure 5). Other than the PMS2 off-target activity, the Hsp90 inhibitors were quite specific for Hsp90.

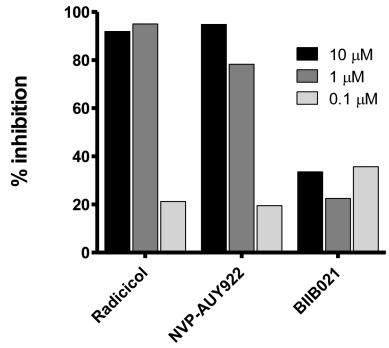

Figure 5. PMS2 is an off-target of Hsp90 inhibitor. NVP-AUY922 and radicicol inhibited the probe labeling of PMS2 in HeLa lysate in a dose-dependent manner.

Profiling Downstream Cellular Effects of Hsp90 Inhibition. Because the ATP acyl phosphate probe enriches several known protein kinase Hsp90 client proteins, it is well suited for profiling the cellular effects of Hsp90 inhibition. Relative to other kinase-focused approaches to identifying Hsp90 client proteins,[24] this method provides additional information in that it also quantifies several ATPases, some of which are known to be affected by Hsp90 inhibition (e.g., Hsp70). Additionally, the profiling experiment can be done such that the lysate retains the inhibitor that has diffused into the cells. In this format, direct target engagement of Hsp90 paralogs can be measured.

In an initial experiment we incubated MCF7 cells with either 80 nM or 1 μM 17-AAG, NVP-AUY922, or DMSO vehicle for 24 h. Following treatment, the cells were harvested and washed and then lysed with a defined amount of buffer. As expected, a large number of protein kinases showed significantly less signal in the compound-treated cells relative to the control cells (Figure 6A). Known Hsp90 client proteins such as Her2 and CHK1 were among the most strongly down-regulated proteins. Only a single protein kinase, Her2, showed a decrease of at least 2-fold at the 80 nM dose of one inhibitor, NVP-AUY922. While the 80 nM dose (in growth media) of NVP-AUY922 constitutes a concentration 10 times its IC_{50} value for Hsp90 binding, the ATPase panel data (Figure 6B) from the same samples only showed about 1.5-fold less signal (~35% inhibition) for labeling of cytosolic Hsp90 relative to control. The 80 nM dose of either compound was insufficient to completely engage the abundant Hsp90 targets, and the partially inhibited Hsp90 activity only resulted in modest effects on the most sensitive client proteins. Comparing the 1 μM doses of 17-AAG and NVP-AUY922 showed a small number of kinases (EphB4, IKKα, ULK1) that were more potently down regulated by NVP-AUY922. Perhaps this was due to the lack of Grp94 or Trap-1 engagement or the weaker inhibition of cytosolic Hsp90 by 17-AAG relative to NVP-AUY922.

DOI: 10.1021/acs.biochem.5b00148
Biochemistry 2015, 54, 3024−3036

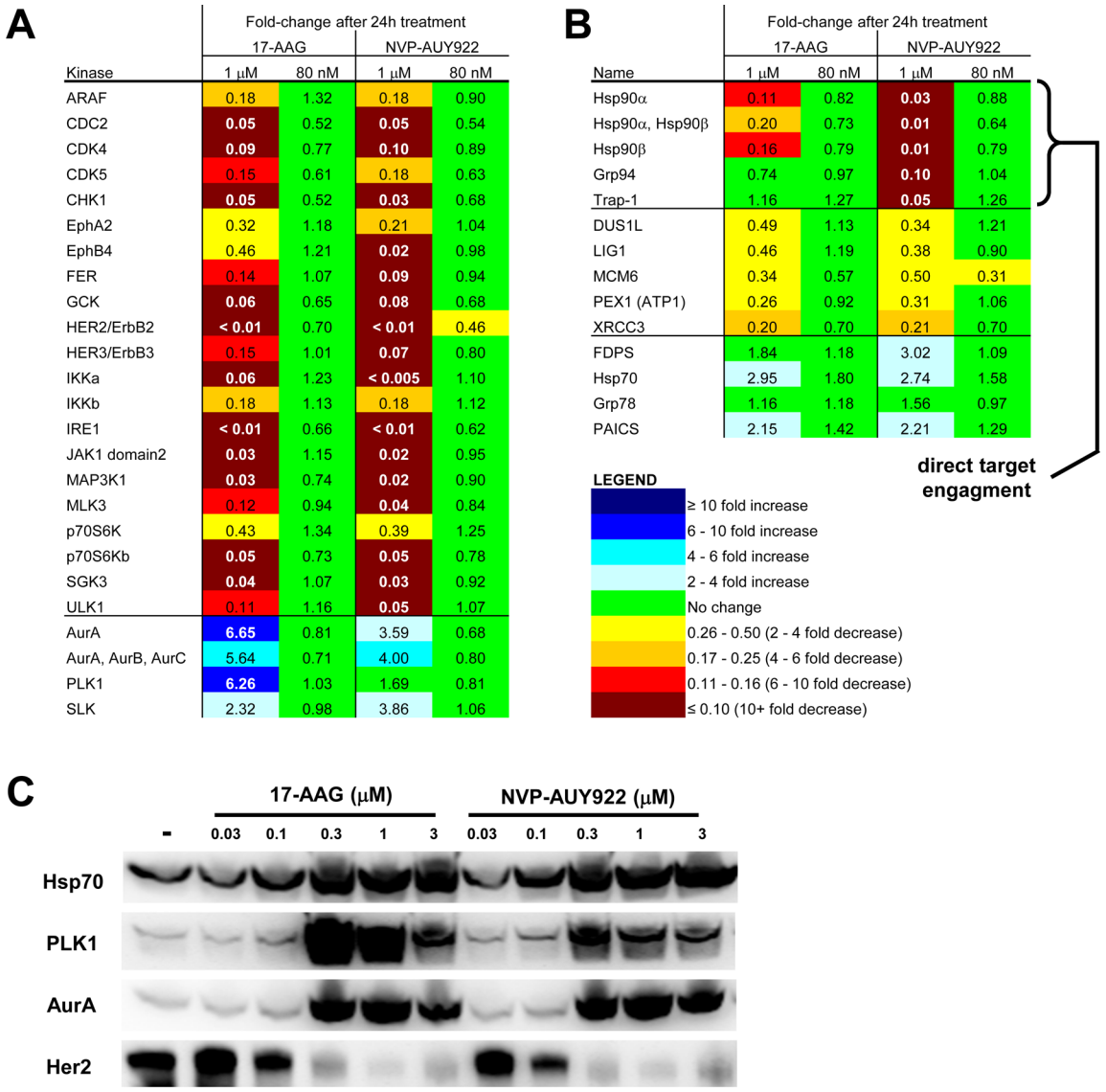

Figure 6. Effects of Hsp90 inhibition on live MCF7 cells. (A) Selected protein kinase profiling results from MCF7 cells treated with Hsp90 inhibitors at 1 μM or 80 nM for 24 h. About 40% of the kinases showed at least a 2-fold decrease in response to Hsp90 inhibition, whereas only a few kinases showed an increase in signal. (B) Selected results from the ATPase panel. The decreased signal from Hsp90 paralogs was due to direct target engagement by inhibitor accumulated in cells during culture. Relatively few ATPases (5%) showed evidence of being an Hsp90 client protein. An expected increase in Hsp70 probe labeling was observed for both inhibitors. See Figure S8, Supporting Information for full protein kinase and ATPase results. (C) Western blots of Hsp70, PLK1, AurA ,and Her2 from treated MCF7 cells. Quantification of the PLK1 signal for treatments with 1 μM 17-AAG or NVP-AUY922 showed a 9.5-fold or 3.4-fold increase, respectively.

As a whole, the kinome of the treated cells was significantly affected: 71 of the 162 protein kinases (44%) detected were decreased at least 2-fold by one of the inhibitors. This sharply contrasted with the results from the ATPase panel, where very few enzymes displayed evidence of being Hsp90 client proteins. Here, only 8 of the 164 ATPases (5%) were down-regulated at least 2-fold. To our knowledge, the most strongly down-regulated ATPase, XRCC3, has not been previously described as an Hsp90 client. One of the hallmarks of Hsp90 inhibition is the up-regulation of Hsp70. As expected, the high dose of both compounds led to a nearly 3-fold increase in Hsp70 probe labeling. A small number of protein kinases were up-regulated in this study, namely, AurA, PLK1, and SLK. Interestingly, the stimulation of PLK1 labeling was much stronger for 1 μM 17-AAG than it was for 1 μM NVP-AUY922. We performed Western blots to confirm the observed increases in AurA, PLK1, and Hsp70 as well as the decrease in Her2, and in all cases this data agreed with the mass spectrometry data (Figure 6C).

Following the MCF7 experiment, we tested the response of A375 cells in culture to 17-AAG and NVP-AUY922 at three concentrations (0.25, 1, and 6.25 μM) and compared two treatment durations, 6 and 24 h. As seen in Figure 7A, the protein kinase profile displayed a similar pattern of kinase down regulation. Several protein kinase client proteins showed decreases at the 6 h time point, and the extent of decrease was generally greater at the 24 h time point. One notable difference was NuaK2, which at 6 h displayed a 3-fold higher signal, but by 24 h had fallen back down to the level of untreated cells. Another kinase that did not follow this pattern is PLK1. It showed an approximately equal level of down-regulation at the 6 and 24 h time points. The effect of Hsp90

DOI: 10.1021/acs.biochem.5b00148
Biochemistry 2015, 54, 3024−3036

A

	Fold-change after 6 h treatment						Fold-change after 24 h treatment					
	17-AAG (μM)			NVP-AUY922 (μM)			17-AAG (μM)			NVP-AUY922 (μM)		
Kinase	6.25	1.25	0.25	6.25	1.25	0.25	6.25	1.25	0.25	6.25	1.25	0.25
CDC2	0.46	0.57	0.73	0.44	0.48	0.64	0.07	0.12	0.49	0.09	0.11	0.13
CDK4	0.05	0.09	0.35	0.07	0.05	0.10	0.02	0.05	0.62	0.02	0.03	0.04
CDK6	< 0.03	< 0.03	0.38	< 0.03	< 0.03	< 0.03	< 0.01	< 0.01	0.51	< 0.01	< 0.01	< 0.01
CHK1	0.44	0.56	0.79	0.50	0.47	0.50	< 0.05	0.10	1.18	< 0.05	< 0.05	0.12
HER3/ErbB3	0.35	0.39	0.55	0.20	0.13	0.23	0.04	0.10	0.71	0.03	0.03	0.05
IKKa	0.29	0.46	1.06	0.36	0.35	0.38	0.01	0.17	0.88	0.01	0.01	0.03
IKKb	0.72	0.74	0.95	0.79	0.67	0.59	0.10	0.35	1.14	0.13	0.14	0.19
JAK1 domain2	0.18	0.14	0.52	0.21	0.20	0.22	< 0.03	< 0.03	0.69	< 0.03	< 0.03	< 0.03
MAP3K1	0.24	0.49	1.13	0.22	0.24	0.13	0.06	0.28	1.25	0.01	0.03	0.09
p70S6K	0.81	0.86	1.01	0.94	0.92	0.96	0.34	0.39	1.21	0.40	0.46	0.43
p70S6Kb	0.70	0.65	0.66	0.75	0.70	0.67	< 0.03	< 0.03	0.60	< 0.03	< 0.03	< 0.03
SGK	< 0.1	0.22	0.68	< 0.1	< 0.1	< 0.1	0.10	0.25	0.83	0.06	0.09	0.11
SGK, SGK2, SGK3	0.50	0.50	0.69	0.56	0.46	0.47	< 0.03	0.11	0.82	< 0.03	< 0.03	0.05
PLK1	0.30	0.61	0.82	0.26	0.28	0.34	0.31	1.05	1.36	0.30	0.45	0.67
AurA	0.65	0.85	0.92	0.76	0.81	0.95	0.89	1.59	1.20	1.01	1.33	1.44
CLK2	ND	ND	ND	ND	ND	ND	1.95	1.60	1.80	2.09	2.41	2.06
NuaK2	2.96	2.48	1.35	2.07	3.16	2.58	0.88	0.83	1.27	1.00	1.23	1.27
SLK	1.04	1.14	1.19	2.18	1.50	1.01	0.81	0.72	1.07	1.69	1.29	1.04

B

	Fold-change after 6 h treatment						Fold-change after 24 h treatment					
	17-AAG (μM)			NVP-AUY922 (μM)			17-AAG (μM)			NVP-AUY922 (μM)		
Name	6.25	1.25	0.25	6.25	1.25	0.25	6.25	1.25	0.25	6.25	1.25	0.25
Hsp90α	0.13	0.22	0.52	< 0.04	< 0.04	< 0.04	0.12	0.26	1.21	< 0.04	< 0.04	< 0.04
Hsp90α, Hsp90β	0.16	0.32	0.73	0.009	0.007	0.01	0.18	0.37	0.81	0.01	0.007	0.01
Hsp90β	0.18	0.32	0.66	0.008	0.006	0.01	0.15	0.33	0.69	0.008	0.006	0.01
Grp94	0.91	0.95	0.98	0.03	0.13	0.73	1.08	0.95	0.99	0.03	0.14	0.75
Trap-1	1.03	1.16	1.10	0.01	0.06	0.48	1.23	1.40	0.91	0.01	0.05	0.55
DCK	1.14	1.20	1.06	0.96	1.21	0.79	0.79	0.56	1.92	0.41	0.38	0.57
DUS1L	0.66	0.88	0.74	0.80	0.79	1.07	0.46	0.51	0.93	0.47	0.60	0.67
MCM6	0.97	0.92	1.06	0.87	0.97	0.93	0.98	0.81	0.97	0.90	0.99	1.03
PMS2	0.66	0.86	1.04	0.21	0.31	1.01	0.91	1.06	0.58	0.25	0.42	0.97
XRCC3	0.64	0.71	0.79	0.76	0.82	0.83	0.23	0.25	0.71	0.38	0.34	0.27
AHCY	1.16	1.34	1.38	1.11	1.24	1.62	2.58	2.08	1.43	2.69	3.19	2.93
FDPS	1.14	1.14	1.15	0.98	1.21	1.17	1.00	0.90	0.99	0.66	0.98	0.92
Hsp70	4.12	4.90	4.02	4.72	3.97	6.04	9.05	8.60	5.05	10.44	9.25	8.54
Grp78	2.11	1.19	1.01	2.17	1.98	1.43	3.02	1.27	0.95	3.83	3.34	1.20
PAICS	1.19	1.11	1.01	0.93	1.14	1.54	2.49	2.32	0.98	2.90	2.48	2.38

Figure 7. Time-dependence of Hsp90 inhibition effects in live A375 cells. (A) Protein kinase panel profiling results in A375 cells treated with the indicated concentration of Hsp90 inhibitor for 6 or 24 h. Nearly all kinases that decreased upon Hsp90 inhibition were further decreased by the longer inhibitor treatment. PLK1 levels decreased in A375, unlike in MCF7. AurA levels remained constant, while a few kinases (NuaK2, CLK2) showed increases. (B) ATPase panel profiling results. A fairly constant level of direct target engagement was observed for all Hsp90 paralogs with both treatment durations. Very few ATPases behaved like Hsp90 client proteins, and only DUS1L and XRCC3 gave similar results in both cell lines. The decrease in PMS2 signal was not time-dependent, consistent with direct inhibition. In addition to Hsp70 induction, the endoplasmic reticulum Hsp70 family member, Grp78, also showed a potent up-regulation. See Figure S9, Supporting Information for full protein kinase and ATPase panel data.

inhibition on the regulation of PLK1 and AurA differed significantly between the A375 and MCF7 cell lines. Whereas both kinases were strongly up-regulated in MCF7 cells, AurA levels remained unchanged and PLK1 showed the aforementioned signal decrease in A375. Because these protein kinases have a prominent role in cell cycle progression, we reasoned that Hsp90 inhibition might have cell-type specific effects on the cell cycle status of these two lines. To test this we treated both cell lines with 5 μM of each inhibitor for 24 h and compared the resulting cell cycle distributions to those of untreated cells using FACS. Indeed, Hsp90 inhibitor treatment altered the cell cycle distributions of both cell types, with A375 cells showing a decrease in cells at the G_0/G_1 phase, whereas MCF7 cells showed an increase in cells at the G_0/G_1 phase (Figure S10, Supporting Information).

The engagement of Hsp90 paralogs by the two inhibitors in A375 cells followed the same pattern as was observed for MCF7 (Figure 7B). NVP-AUY922 strongly inhibited all four paralogs and showed overall greater potency than 17-AAG, which only inhibited cytosolic Hsp90 paralogs. For both compounds the extent of engagement did not differ between the 6 and 24 h time points. Considering that 6 h should be a long enough incubation time for the intracellular concentration of inhibitor to reach equilibrium, the lack of time-dependence in the observed signal loss is understandable for a directly inhibited target enzyme. In A375 cells the off-target ATPase PMS2 was detected, and it only showed inhibition by NVP-AUY922. Like the Hsp90 paralogs, the extent of inhibition did not increase with longer inhibitor treatment. Of the ATPase Hsp90 client proteins detected, again XRCC3 showed the most significant decrease, with the response only being evident at the

DOI: 10.1021/acs.biochem.5b00148
Biochemistry 2015, 54, 3024−3036

24 h time point. The induction of Hsp70 was readily apparent at the 6 h time point and increased in magnitude at the 24 h time point. At both time points the up-regulation of Hsp70 was observed even for the lowest concentration of 17-AAG where Hsp90 engagement was incomplete. Additionally, the levels of the endoplasmic reticulum Hsp70 paralog, Grp78, were increased in A375, an effect not observed in MCF7. Another distinction between the two cell types was the observed up-regulation of adenosylhomocysteinase (AHCY) by both Hsp90 inhibitors in A375. While we have not yet investigated how AHCY activity might play a role in the cellular response to Hsp90 inhibition, this observation highlights how the reactivity of the ATP acyl phosphate probe can reveal unexpected responses in a diverse range of enzyme types.

DISCUSSION

A variety of ATPases have generated intense interest as drug targets, particularly members of the heat shock protein families.[25] The mass spectrometry chemoproteomics platform presented here takes advantage of the broad reactivity of an ATP acyl phosphate probe to enable the profiling of a diverse set of ATPases, including the prominent drug target, Hsp90. When combined with the previously described protein kinase profiling technology, this approach provides a quantitative measure of inhibition levels for several hundred protein kinases and ATPases in a single experiment. While the number of targets profiled is heavily influenced by the pattern of protein expression observed in specific cell types, the only limitation to the source of proteome to be profiled is the availability of protein sequence data. Here, we have primarily discussed results from human cancer cell lines, but we have also profiled Hsp90 and other ATPases in human blood cell samples, a variety of mouse and rat tissues, and bacterial cell lysates. Unlike other methods for assaying Hsp90 in native conditions where protein−protein interactions are preserved, this strategy does so while maintaining the capacity to distinctly measure inhibition of individual Hsp90 paralogs.

The use of native cellular lysates allows the relative inhibition of each Hsp90 paralog to be measured at their natural relative abundances as they compete with each other for compound binding. Additionally, within the context of a complete proteome the effects of nonspecific protein binding and off-target inhibition on the available inhibitor concentration are generally accounted for. Our results indicate that the aggregate Hsp90 inhibitor binding capacity of a typical proteome far exceeds the published IC_{50} concentration for all of the inhibitors we profiled. The abundance of cytosolic Hsp90 paralogs has been widely discussed in the literature,[26] and Grp94 is known to be highly abundant also.[27] In fact, based on mass spectrometry signal, Grp94 appears to be the most abundant protein that is labeled by the ATP probe. For an inhibitor like NVP-AUY922 that has high affinity for all four Hsp90 paralogs, this means that a sizable compound dose (relative to IC_{50}) is needed to attain a substantial level of inhibition of any one Hsp90 paralog. The consequences of Hsp90 paralog abundance were clearly observed in the MCF7 live cell treatment study. When cells were treated with 80 nM NVP-AUY922, the level of inhibition was very low for all Hsp90 paralogs and the overall cellular response was limited. Therefore, if a desired biological response is dependent upon a high degree of inhibition of a specific Hsp90 paralog, a weakly potent but highly paralog-specific Hsp90 inhibitor should be more beneficial than a highly potent, but nonspecific inhibitor. Regardless of the compound specificity, it seems likely that inhibitor dosing regimens capable of yielding cellular compound concentrations significantly higher than low nanomolar levels are needed to fully engage any Hsp90 paralog.

The reactivity of the ATP acyl phosphate probe offers a unique opportunity to discover unexpected ATP-binding sites. The use of native cellular proteomes helps enable such discoveries, as in the recently published example of the ATP-binding site formed by the protein−protein interface of the p38α:mapkap kinase 2/3 heterodimer.[28] ATP probe binding to this site requires heterodimer formation and leads to the acylation of Lys-15 of p38α in a region of the kinase some distance from the canonical ATP-binding site. For Hsp90, the probe labeling of lysine residues from the middle domain was unanticipated. While the middle domain has a known role in ATP hydrolysis, the isolated N-terminal domain is sufficient for ATP-binding.[29] The full-length yeast enzyme in complex with AMPPNP and the cochaperone Sba1(p23) shown in Figure 2B is the only known structure of a full-length eukaryotic cytosolic Hsp90. (Hundreds of isolated N-terminal domain structures have been determined.) In this conformation the middle domain labeling site, Lys-335 (yeast numbering, equivalent to Lys-347 of human Hsp90β) is located a significant distance (>30 Å) from the bound nucleotide. In contrast, the N-terminal domain labeling site (Lys-97) is located directly adjacent to the ATP analogue. All of the inhibitors examined in this study are known to bind within the N-terminal ATP-binding site. Thus, their capacity to prevent the acylation of lysine residues in this site is consistent with a mechanism of competitively inhibiting probe binding to the same site. The observation of equipotent inhibition of both N-terminal and middle domain probe labeling for all combinations of Hsp90 paralog and inhibitor or ATP can be most readily explained by a model in which all probe labeling is mediated by probe bound to the N-terminal binding site.

While current structures of full-length Hsp90s do not reveal how a probe bound to the N-terminal domain could label a distant lysine in the middle domain, the conservation of this observation for different human Hsp90 paralogs, Hsp90s from other eukaryotes and even bacterial Hsp90s suggests that the capacity is inherent to the protein itself. Many Hsp90 client proteins are themselves ATP-binding proteins and perhaps could form an interfacial ATP-binding site near the middle domain of Hsp90 when bound as a substrate. However, the variability of client proteins from paralog to paralog and especially from human to bacteria makes the likelihood of client protein-mediated probe labeling less probable. The same rationale seems reasonable to apply toward Hsp90-*co*-chaperone complexes as well, given that Hsp90 paralogs sequestered in different cellular compartments (cytosol, ER, mitochondria) each have unique cochaperones. Additionally, it is not known whether inhibitor binding would prevent formation of Hsp90-*co*-chaperone complexes and any resulting interfacial ATP-binding sites. Most importantly, any probe labeling mechanism that involves a second, independent binding site for the ATP probe (or ATP itself) would require that the secondary site of each paralog to coincidentally have affinity for each Hsp90 inhibitor equal to the affinity in the primary ATP-binding site to explain our observations of equipotent inhibition for both N-terminal and middle domain labeling. The greater simplicity of a model invoking only the currently known ATP-binding site as the basis for the probe

DOI: 10.1021/acs.biochem.5b00148
Biochemistry 2015, 54, 3024−3036

labeling of the middle domain of Hsp90 makes it our favored explanation.

For the middle domain labeling reaction to occur, the conformation observed in the structure of the yeast full-length enzyme must undergo a significant rearrangement placing the loop containing Lys-335 in the vicinity of bound ATP. Considering the known conformational flexibility of Hsp90 paralogs[15] and the documented difficulty in crystallizing full-length Hsp90 presumably due to its inherent mobility,[30] such a rearrangement is reasonable to envision. The probe-based assay likely assesses a native conformation of Hsp90 that has not yet been observed by crystallography. Notably, the loop containing Lys-335 in the yeast Hsp90 structure is disordered in one of the two protomers. The equivalent loops from the only other two crystal structures of full-length eukaryotic Hsp90 paralogs (canine Grp94 and zebrafish Trap-1) are also disordered in either one or both of their respective subunits.[31,32] These findings suggest that this region of Hsp90 is intrinsically conformationally flexible, and this characteristic is conserved across a broad range of species and among the various Hsp90 paralogs. Potentially, the binding of substrates to HSP90 may induce a conformational change that brings Lys-335 in close proximity to the ATP binding site in the N-terminal domain. Alternatively, we cannot rule out the possibility that native HSP90 participates in higher order multimeric structures not yet captured in existing crystallographic structures in which the middle domain lysine residue in one monomer is in close proximity to the ATP binding site of another monomer. Regardless as to the specific model, ATP-competitive middle domain labeling is observed in human, mouse, and rat cytosolic Hsp90, Grp94, and mitochondrial Trap-1s as well as the related bacterial Hsp90s from *E. coli* and *P. aeruginosa*.

A conformational rearrangement that places the middle domain loop containing the ATP probe labeling sites in close proximity to the N-terminal ATP-binding site could function as a mechanism to couple the energy from ATP hydrolysis to the conformational maturation of bound client proteins. The stretch of consecutive positively charged amino acids in this loop could promote this transition via an electrostatic interaction with the triphosphate of ATP. The data suggest that the first positively charged residue from either the loop in Hsp90α (Arg-355) or Hsp90β (Lys-347) is the primary mediator of the interaction between the loop and bound ATP (or probe). Considering that the identity of this amino acid is not conserved between the two paralogs, a direct role in the catalysis of ATP hydrolysis seems unlikely. Some plasticity in the chemical mechanism allowing for either arginine or lysine to serve the same catalytic role is in theory possible; however, any direct evidence indicating such a role is currently lacking. For Hsp90α, Hsp90β, and Grp94 multiple lysines from the middle domain loop are able to interact with bound probe, as they all showed labeling and equipotent sensitivity to inhibition. Perhaps the precise orientation of the loop−ATP interaction varies depending on the size or shape of a bound client protein. Having multiple positively charged residues could help maintain the chaperone function of Hsp90 for a diverse set of client proteins.

Only a limited number of earlier studies have tested Hsp90 inhibitors for off-target activity against other ATPases, perhaps due to the technical challenges inherent in assaying a diverse set of enzymes. The structurally unrelated but functionally similar ATPase, Hsp70, has been shown not to be a target of some Hsp90 inhibitors.[33,34] Additionally, the GHKL superfamily member, human DNA topoisomerase II, has warranted some attention, and radicicol was found to inhibit the DNA relaxation and decatenation activities, albeit at a concentration of 100 μM.[35] Here, the broad profiling capacity of the chemoproteomics platform enabled the detection of a novel off-target of two of the Hsp90 inhibitors; radicicol and NVP-AUY922 inhibited probe labeling of PMS2. PMS2 is an ATPase that forms a heterodimer with another MutL homologue, MLH1, and together they function in DNA mismatch repair. It is likely that inhibition of PMS2 would be undesirable as mutations in both PMS2 and MLH1 are directly linked to the incidence of hereditary nonpolyposis colon cancer.[36] While both compounds were less active against PMS2 than they were against Hsp90, the autosomal dominant nature of the disease may mean that even partial loss of PMS2 activity would be deleterious. If high doses of an Hsp90 inhibitor are needed to achieve a significant level of Hsp90 inhibition, as observed in the live cell treatment studies, then partial inhibition of off-targets like PMS2 would be more likely. In clinical trials, Hsp90 inhibitors have suffered from several types of toxicities, including hepatic, gastrointestinal, and ocular.[37] The reasons for these toxicities are not fully understood. While certain examples, like the hepatotoxicity of 17-AAG, are unlikely to be related to PMS2 inhibition based on our work, the prospect of off-target inhibition leading to other cases of toxicity warrants consideration. The same inhibitors can show varied effects in different cell types, as evidenced by the cell cycle status differences seen in MCF7 and A375 cells treated with Hsp90 inhibitors. Perhaps, a greater understanding of toxicity would be facilitated by measurement of on- and off-target engagement in relevant tissue samples from inhibitor-treated animals or patients.

The ATP acyl phosphate probe provides a favorable balance between being specifically recognized by enzyme active sites and having high reactivity toward lysine residues in a broad spectrum of enzyme targets. The diverse range of ATPases and protein kinases amenable to profiling with this system allows for the detection of small molecule−protein interactions for several targets that would otherwise be difficult to conveniently assay. The biochemical activity of the ATPase PMS2 has only been studied to a limited extent, and to our knowledge, no small molecule inhibitors were known previous to the current findings of inhibition by radicicol and NVP-AUY922. Because the probe-labeling reaction occurs in solution and in the presence of natural mixtures of proteins, it can assess protein conformations and complexes that are inaccessible to other methods of study. This enabled the discovery of a novel, but highly conserved, conformational state of Hsp90 during its complex catalytic cycle.

■ ASSOCIATED CONTENT

Supporting Information

Additional materials and methods, detailed discussion of the analysis of labeled peptides derived from Asp-N digests and the results from profiling experiments performed at different proteome concentrations, a full list of nonprotein kinase ATPases that can be profiled with the chemoproteomics platform, complete tables of percent inhibition values and calculated IC_{50} values from ATP and inhibitor profiling, complete protein kinase and ATPase panel data from lysate and live-cell treatment studies, and cell cycle analysis figures. The Supporting Information is available free of charge on the

DOI: 10.1021/acs.biochem.5b00148
Biochemistry 2015, 54, 3024−3036

ACS Publications website at DOI: 10.1021/acs.biochem.5b00148.

AUTHOR INFORMATION

Corresponding Author

*E-mail: johnk@activx.com. Phone: 858-526-2502. Fax: 858-587-4878.

Notes

The authors declare no competing financial interest.

ABBREVIATIONS

Hsp90, heat shock protein 90; LC-MS/MS, liquid chromatography tandem mass spectrometry; GHKL, gyrase-Hsp90-histidine kinase-mutL superfamily; AUC, area under the curve; 17-AAG, 17-allylamino-17-desmethoxygeldanamycin

REFERENCES

(1) Cravatt, B. F., Wright, A. T., and Kozarich, J. W. (2008) Activity-based protein profiling: from enzyme chemistry to proteomic chemistry. *Annu. Rev. Biochem. 77*, 383−414.

(2) Patricelli, M. P., Szardenings, A. K., Liyanage, M., Nomanbhoy, T. K., Wu, M., Weissig, H., Aban, A., Chun, D., Tanner, S., and Kozarich, J. W. (2007) Functional interrogation of the kinome using nucleotide acyl phosphates. *Biochemistry 46*, 350−358.

(3) Patricelli, M. P., Nomanbhoy, T. K., Wu, J., Brown, H., Zhou, D., Zhang, J., Jagannathan, S., Aban, A., Okerberg, E., Herring, C., Nordin, B., Weissig, H., Yang, Q., Lee, J.-D., Gray, N. S., and Kozarich, J. W. (2011) In situ kinase profiling reveals functionally relevant properties of native kinases. *Chem. Biol. 18*, 699−710.

(4) Chen, B., Zhong, D., and Monteiro, A. (2006) Comparative genomics and evolution of the HSP90 family of genes across all kingdoms of organisms. *BMC Genomics 7*, 156.

(5) Sepp-Lorenzino, L., Ma, Z., Lebwohl, D. E., Vinitsky, A., and Rosen, N. (1995) Herbimycin A induces the 20 S proteasome- and ubiquitin-dependent degradation of receptor tyrosine kinases. *J. Biol. Chem. 270*, 16580−16587.

(6) Sharma, K., Vabulas, R. M., Macek, B., Pinkert, S., Cox, J., Mann, M., and Hartl, F. U. (2012) Quantitative proteomics reveals that Hsp90 inhibition preferentially targets kinases and the DNA damage response. *Mol. Cell. Proteomics 11*, M111.014654.

(7) Bergerat, A., de Massy, B., Gadelle, D., Varoutas, P. C., Nicolas, A., and Forterre, P. (1997) An atypical topoisomerase II from Archaea with implications for meiotic recombination. *Nature 386*, 414−417.

(8) Dutta, R., and Inouye, M. (2000) GHKL, an emergent ATPase/kinase superfamily. *Trends Biochem. Sci.*, 24−28.

(9) Chen, B., Piel, W. H., Gui, L., Bruford, E., and Monteiro, A. (2005) The HSP90 family of genes in the human genome: insights into their divergence and evolution. *Genomics 86*, 627−637.

(10) Sciacovelli, M., Guzzo, G., Morello, V., Frezza, C., Zheng, L., Nannini, N., Calabrese, F., Laudiero, G., Esposito, F., Landriscina, M., Defilippi, P., Bernardi, P., and Rasola, A. (2013) The mitochondrial chaperone TRAP1 promotes neoplastic growth by inhibiting succinate dehydrogenase. *Cell Metab. 17*, 988−999.

(11) Immormino, R. M., Metzger, L. E., Reardon, P. N., Dollins, D. E., Blagg, B. S. J., and Gewirth, D. T. (2009) Different poses for ligand and chaperone in inhibitor-bound Hsp90 and GRP94: implications for paralog-specific drug design. *J. Mol. Biol. 388*, 1033−1042.

(12) Duerfeldt, A. S., Peterson, L. B., Maynard, J. C., Ng, C. L., Eletto, D., Ostrovsky, O., Shinogle, H. E., Moore, D. S., Argon, Y., Nicchitta, C. V., and Blagg, B. S. J. (2012) Development of a Grp94 inhibitor. *J. Am. Chem. Soc. 134*, 9796−9804.

(13) Kang, B. H., Plescia, J., Song, H. Y., Meli, M., Colombo, G., Beebe, K., Scroggins, B., Neckers, L., and Altieri, D. C. (2009) Combinatorial drug design targeting multiple cancer signaling networks controlled by mitochondrial Hsp90. *J. Clin. Invest. 119*, 454−464.

(14) Ernst, J. T., Liu, M., Zuccola, H., Neubert, T., Beaumont, K., Turnbull, A., Kallel, A., Vought, B., and Stamos, D. (2014) Correlation between chemotype-dependent binding conformations of HSP90α/β and isoform selectivity-Implications for the structure-based design of HSP90α/β selective inhibitors for treating neurodegenerative diseases. *Bioorg. Med. Chem. Lett. 24*, 204−208.

(15) Mayer, M. P. (2010) Gymnastics of molecular chaperones. *Mol. Cell 39*, 321−331.

(16) Taldone, T., Patel, P. D., Patel, M., Patel, H. J., Evans, C. E., Rodina, A., Ochiana, S., Shah, S. K., Uddin, M., Gewirth, D., and Chiosis, G. (2013) Experimental and Structural Testing Module to Analyze Paralogue-Specificity and Affinity in the Hsp90 Inhibitors Series. *J. Med. Chem. 56*, 6803−6818.

(17) Stebbins, C. E., Russo, a a, Schneider, C., Rosen, N., Hartl, F. U., and Pavletich, N. P. (1997) Crystal structure of an Hsp90-geldanamycin complex: targeting of a protein chaperone by an antitumor agent. *Cell 89*, 239−250.

(18) Ali, M. M. U., Roe, S. M., Vaughan, C. K., Meyer, P., Panaretou, B., Piper, P. W., Prodromou, C., and Pearl, L. H. (2006) Crystal structure of an Hsp90-nucleotide-p23/Sba1 closed chaperone complex. *Nature 440*, 1013−1017.

(19) Sharp, S. Y., Prodromou, C., Boxall, K., Powers, M. V., Holmes, J. L., Box, G., Matthews, T. P., Cheung, K.-M. J., Kalusa, A., James, K., Hayes, A., Hardcastle, A., Dymock, B., Brough, P. a, Barril, X., Cansfield, J. E., Wright, L., Surgenor, A., Foloppe, N., Hubbard, R. E., Aherne, W., Pearl, L., Jones, K., McDonald, E., Raynaud, F., Eccles, S., Drysdale, M., and Workman, P. (2007) Inhibition of the heat shock protein 90 molecular chaperone in vitro and in vivo by novel, synthetic, potent resorcinylic pyrazole/isoxazole amide analogues. *Mol. Cancer Ther. 6*, 1198−211.

(20) Roe, S. M., Prodromou, C., O'Brien, R., Ladbury, J. E., Piper, P. W., and Pearl, L. H. (1999) Structural Basis for Inhibition of the Hsp90 Molecular Chaperone by the Antitumor Antibiotics Radicicol and Geldanamycin. *J. Med. Chem. 42*, 260−266.

(21) Shi, J., Van de Water, R., Hong, K., Lamer, R. B., Weichert, K. W., Sandoval, C. M., Kasibhatla, S. R., Boehm, M. F., Chao, J., Lundgren, K., Timple, N., Lough, R., Ibanez, G., Boykin, C., Burrows, F. J., Kehry, M. R., Yun, T. J., Harning, E. K., Ambrose, C., Thompson, J., Bixler, S. a, Dunah, A., Snodgrass-Belt, P., Arndt, J., Enyedy, I. J., Li, P., Hong, V. S., McKenzie, A., and Biamonte, M. a. (2012) EC144 is a potent inhibitor of the heat shock protein 90. *J. Med. Chem. 55*, 7786−7795.

(22) Eccles, S. a, Massey, A., Raynaud, F. I., Sharp, S. Y., Box, G., Valenti, M., Patterson, L., de Haven Brandon, A., Gowan, S., Boxall, F., Aherne, W., Rowlands, M., Hayes, A., Martins, V., Urban, F., Boxall, K., Prodromou, C., Pearl, L., James, K., Matthews, T. P., Cheung, K.-M., Kalusa, A., Jones, K., McDonald, E., Barril, X., Brough, P. a, Cansfield, J. E., Dymock, B., Drysdale, M. J., Finch, H., Howes, R., Hubbard, R. E., Surgenor, A., Webb, P., Wood, M., Wright, L., and Workman, P. (2008) NVP-AUY922: a novel heat shock protein 90 inhibitor active against xenograft tumor growth, angiogenesis, and metastasis. *Cancer Res. 68*, 2850−2860.

(23) Lundgren, K., Zhang, H., Brekken, J., Huser, N., Powell, R. E., Timple, N., Busch, D. J., Neely, L., Sensintaffar, J. L., Yang, Y., McKenzie, A., Friedman, J., Scannevin, R., Kamal, A., Hong, K., Kasibhatla, S. R., Boehm, M. F., and Burrows, F. J. (2009) BIIB021, an orally available, fully synthetic small-molecule inhibitor of the heat shock protein Hsp90. *Mol. Cancer Ther. 8*, 921−929.

(24) Haupt, A., Joberty, G., Bantscheff, M., Fröhlich, H., Stehr, H., Schweiger, M. R., Fischer, A., Kerick, M., Boerno, S. T., Dahl, A., Lappe, M., Lehrach, H., Gonzalez, C., Drewes, G., and Lange, B. M. (2012) Hsp90 inhibition differentially destabilises MAP kinase and TGF-beta signalling components in cancer cells revealed by kinase-targeted chemoproteomics. *BMC Cancer 12*, 38.

(25) Massey, A. J. (2010) ATPases as drug targets: insights from heat shock proteins 70 and 90. *J. Med. Chem. 53*, 7280−7286.

(26) Subbarao Sreedhar, A., Kalmár, É., Csermely, P., and Shen, Y.-F. (2004) Hsp90 isoforms: functions, expression and clinical importance. *FEBS Lett. 562*, 11−15.

DOI: 10.1021/acs.biochem.5b00148
Biochemistry 2015, 54, 3024−3036

(27) Mao, C., Wang, M., Luo, B., Wey, S., Dong, D., Wesselschmidt, R., Rawlings, S., and Lee, A. S. (2010) Targeted mutation of the mouse Grp94 gene disrupts development and perturbs endoplasmic reticulum stress signaling. *PLoS One 5*, e10852.
(28) Okerberg, E. S., Brown, H. E., Minimo, L., Alemayehu, S., Rosenblum, J., Patricelli, M., Nomanbhoy, T., and Kozarich, J. W. (2014) Monitoring native p38α:MK2/3 complexes via trans delivery of an ATP acyl phosphate probe. *J. Am. Chem. Soc. 136*, 4664−4669.
(29) Grenert, J. P., Sullivan, W. P., Fadden, P., Haystead, T. A., Clark, J., Mimnaugh, E., Krutzsch, H., Ochel, H. J., Schulte, T. W., Sausville, E., Neckers, L. M., and Toft, D. O. (1997) The amino-terminal domain of heat shock protein 90 (hsp90) that binds geldanamycin is an ATP/ADP switch domain that regulates hsp90 conformation. *J. Biol. Chem. 272*, 23843−23850.
(30) Meyer, P., Prodromou, C., Hu, B., Vaughan, C., Roe, S. M., Panaretou, B., Piper, P. W., and Pearl, L. H. (2003) Structural and functional analysis of the middle segment of hsp90: implications for ATP hydrolysis and client protein and cochaperone interactions. *Mol. Cell 11*, 647−658.
(31) Dollins, D. E., Warren, J. J., Immormino, R. M., and Gewirth, D. T. (2007) Structures of GRP94-nucleotide complexes reveal mechanistic differences between the hsp90 chaperones. *Mol. Cell 28*, 41−56.
(32) Lavery, L. a, Partridge, J. R., Ramelot, T. a, Elnatan, D., Kennedy, M. a, and Agard, D. a. (2014) Structural asymmetry in the closed state of mitochondrial Hsp90 (TRAP1) supports a two-step ATP hydrolysis mechanism. *Mol. Cell 53*, 330−343.
(33) Massey, A. J., Schoepfer, J., Brough, P. a, Brueggen, J., Chène, P., Drysdale, M. J., Pfaar, U., Radimerski, T., Ruetz, S., Schweitzer, A., Wood, M., Garcia-Echeverria, C., and Jensen, M. R. (2010) Preclinical antitumor activity of the orally available heat shock protein 90 inhibitor NVP-BEP800. *Mol. Cancer Ther. 9*, 906−919.
(34) Menezes, D. L., Taverna, P., Jensen, M. R., Abrams, T., Stuart, D., Yu, G. K., Duhl, D., Machajewski, T., Sellers, W. R., Pryer, N. K., and Gao, Z. (2012) The novel oral Hsp90 inhibitor NVP-HSP990 exhibits potent and broad-spectrum antitumor activities in vitro and in vivo. *Mol. Cancer Ther. 11*, 730−739.
(35) Gadelle, D., Graille, M., and Forterre, P. (2006) The HSP90 and DNA topoisomerase VI inhibitor radicicol also inhibits human type II DNA topoisomerase. *Biochem. Pharmacol. 72*, 1207−1216.
(36) Guarné, a, Junop, M. S., and Yang, W. (2001) Structure and function of the N-terminal 40 kDa fragment of human PMS2: a monomeric GHL ATPase. *EMBO J. 20*, 5521−5531.
(37) Fogliatto, G., Gianellini, L., Brasca, M. G., Casale, E., Ballinari, D., Ciomei, M., Degrassi, A., De Ponti, A., Germani, M., Guanci, M., Paolucci, M., Polucci, P., Russo, M., Sola, F., Valsasina, B., Visco, C., Zuccotto, F., Donati, D., Felder, E., Pesenti, E., Galvani, A., Mantegani, S., and Isacchi, A. (2013) NMS-E973, a novel synthetic inhibitor of Hsp90 with activity against multiple models of drug resistance to targeted agents, including intracranial metastases. *Clin. Cancer Res. 19*, 3520−3532.

DOI: 10.1021/acs.biochem.5b00148
Biochemistry 2015, 54, 3024−3036